Activation Analysis for the ITER Divertor Cassette

H.Y. Khater and M.E. Sawan

June 1998

UWFDM-1083

Presented at the 13th Topical Meeting on the Technology of Fusion Energy, June 7–11, 1998, Nashville TN

FUSION TECHNOLOGY INSTITUTE
UNIVERSITY OF WISCONSIN
MADISON WISCONSIN

ACTIVATION ANALYSIS FOR THE ITER DIVERTOR CASSETTE

H. Y. Khater and M. E. Sawan
Fusion Technology Institute
University of Wisconsin-Madison
Madison, Wisconsin 53706, USA
(608) 263-2167

ABSTRACT

A detailed three-dimensional model (3-D) has been developed for the divertor cassette in the ITER design. The layered configurations of the dome PFC and vertical targets were modeled accurately with the front tungsten layer modeled separately. 3-D neutronics calculations have been performed to determine the detailed spatial distribution of the neutron flux in the divertor cassette. A detailed activation analysis has been performed for zones representing the different critical components of the divertor cassette. The calculations have been performed for two operational scenarios. Special attention has been given to the top 1 cm tungsten layer of the divertor dome. The radioactivity generated in the tungsten layers of the divertor is mostly dominated by ^{187}W during the first day after shutdown. The GlidCop copper and 316 SS-LN parts of the divertor also generated considerable levels of activity and decay heat. Nevertheless, the analysis showed that the tungsten Plasma Facing Component (PFC) is clearly the most critical part of the divertor from the decay heat generation point of view.

I. INTRODUCTION

The ITER divertor cassette design went through several changes to improve its performance[1]. The design utilizes 60 divertor cassettes with vertical targets and a central dome. These cassettes are exposed to direct source neutrons coming from the plasma as well as secondary lower energy neutrons resulting from neutron interactions in the cassettes themselves and other in-vessel components. Knowledge of the amount of radioactivity and decay heat produced by these neutrons in the different components of the divertor cassette is essential for proper safety and environmental analysis. Due to the geometrical complexity of the divertor region, three-dimensional analyses are required to account for the effects of the geometrical details on the neutron flux. 3-D neutronics calculations were performed for the divertor region to determine the nuclear parameters in the divertor cassette. The neutron spectra in the divertor zones are used in the activation calculations. The activation calculations are performed for two operational scenarios to determine the level of activity and decay heat generated in the different zones of the divertor.

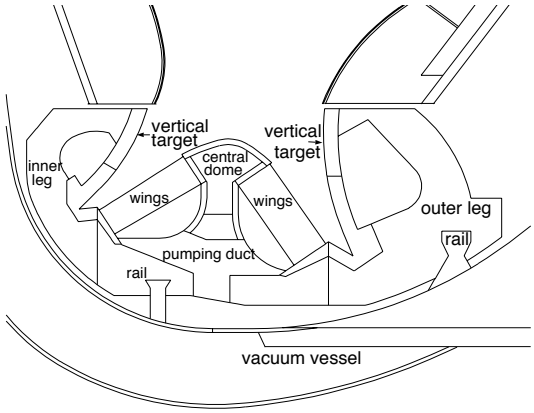

Fig. 1. Vertical cross section at middle of cassette model.

II. 3-D CALCULATIONAL MODEL

The continuous energy, coupled neutron-gamma ray Monte Carlo code MCNP-4A[2] has been used in the 3-D neutron transport calculations. The nuclear data used is based on the FENDL-1 evaluation[3]. The detailed geometrical configuration of the divertor cassette has been modeled for 3-D neutronics calculations. The model represents a nine degree toroidal sector of ITER. Hence, it includes one and a half cassettes with the associated nominal 1 cm gaps between adjacent cassettes. The model includes in detail the high heat flux plasma facing components, the vertical targets, the wings with associated plates, and the gas boxes, as well as the central dome and cassette bodies. The 37.5 cm wide and 17.5 cm thick divertor pumping duct at the bottom of each cassette is included in the model. The rails upon which the cassettes move toroidally during maintenance are also included. Each divertor cassette in the model was divided into 103 regions to provide detailed spatial distribution of the neutron flux. The layered configurations of the dome PFC and vertical targets were modeled accurately with the front tungsten layer modeled separately. This was

essential to properly account for self-shielding effects of the giant resonance for ^{186}W at 20 eV that produces ^{187}W which dominates decay heat in the W PFC. Separate regions are included in the model to represent the mechanical attachments and coolant pipe connections for the dome, vertical targets, and wings. Fig. 1 shows a vertical cross section of the cassette model at a toroidal location at the center of the cassette through the pumping ducts. Compositions of material used in the analysis include all expected impurities[1].

III. ACTIVATION CALCULATION

A detailed activation analysis is performed using the latest version of the activation code DKR-PULSAR2.0[4]. The code combined the 175-group neutron flux calculated by the MCNP-4A code with the FENDL/A-2.0 and FENDL/D-2.0 data libraries[5] to calculate the activity and decay heat generated in the different zones of the divertor. Special attention was given to the top 1 cm tungsten layer of the divertor dome. A correct treatment of the tungsten self-shielding problem was taken into account by replacing the $^{186}W(n,\gamma)$ cross section in the FENDL/A-2.0 library with the effective cross section calculated from the MCNP-4A calculations. Even though the neutron capture cross sections of ^{182}W and ^{183}W also have significant resonances in the thermal energy range, results presented in this paper are focused only on correcting for the $^{186}W(n,\gamma)$ self-shielding effect[6]. That is due to the fact that the daughters of ^{182}W and ^{183}W are mostly short lived with minor impact on the total decay heat generation in the tungsten layer.

The level of activation induced in the divertor is dependent on operation time as well as the corresponding fluence. The choice of pulsing sequences, including dwell times, used in activation analysis is also of great importance to safety analysis. Using a detailed and accurate pulsing sequence is required to obtain an accurate picture of the possible safety hazard posed by the irradiated structure of the divertor in the case of the accidental release of some of its radioactive inventory. In addition, a reliable estimate of the level of decay heat generated in the divertor is needed to accurately calculate the expected temperature rise of its structure during a Loss of Coolant Accident (LOCA) and/or a Loss of Flow Accident (LOFA). This temperature rise would also influence the level of possible radioactive release during a severe accident. To examine the effect of pulsing sequences on the decay heat generation, the calculations were performed for the following two operational scenarios:

1. SA1: This scenario corresponds to a total machine fluence of 0.3 MWa/m^2. It has a long term availability of 25% and a final month availability of 50%. A burn pulse length of one hour producing 1500 MW of fusion power is used in this scenario.

2. M5: This scenario corresponds to a total fluence of 0.1 MWa/m^2. It has a long term availability of only 4% and a last month availability of 50%. A 1000 second burn producing 1500 MW of fusion power is used.

IV. ACTIVATION RESULTS

Activation and decay heat values are calculated for 12 different times following shutdown, ranging from zero to 1000 years. The same calculational approach is used with the two operational scenarios previously discussed. Results are summarized here for selected zones with materials contained in each zone given between brackets. These zones represent areas of largest flux and activation in each component. The detailed results are given in a separate ITER report[6].

a. Dome PFC:

• Zone 1 (100% W)

This zone represents the top 1 cm tungsten PFC layer of the divertor dome. ^{183m}W ($T_{1/2}$ = 5.2 s) is the dominant contributor to the activity induced at shutdown for both operational scenarios. The ^{187}W ($T_{1/2}$ = 23.9 h) is the other major contributor to activity. During the first day following shutdown, ^{187}W and ^{185}W ($T_{1/2}$ = 75.1 d) dominate the induced activity. ^{185}W and ^{181}W are the major contributors to activity one year following shutdown. At 10 years following shutdown, ^{179}Ta ($T_{1/2}$ = 665 d) generates more than 60% of the zone's activity. ^{60}Co ($T_{1/2}$ = 5.27 y) is the other major contributor to activity at the same time. Activities induced for times greater than 10 years are dominated by ^{39}Ar ($T_{1/2}$ = 269 y), ^{63}Ni ($T_{1/2}$ = 100 y), ^{91}Nb ($T_{1/2}$ = 10,000 y), and ^{14}C ($T_{1/2}$ = 5730 y). All tungsten radionuclides are generated by (n,γ) and (n,2n) reactions with natural tungsten included in the calculation. All other contributors to activity following shutdown are produced by nuclear interactions with impurities included in the tungsten chemical composition. ^{179}Ta is produced by the $^{180}Ta(n,2n)$ reaction, ^{60}Co is produced by $^{59}Co(n,\gamma)$ reaction, ^{39}Ar is mostly produced via the $^{39}K(n,p)$ pathway, ^{63}Ni is mostly generated by the $^{62}Ni(n,\gamma)$ reaction, ^{91}Nb is produced by the $^{92}Mo(n,d)$ pathway, and ^{14}C is largely generated by the $^{14}N(n,\gamma)$ reaction. The chemical composition of the tungsten alloy used in this analysis contains as impurities 10 wppm each of tantalum, cobalt, potassium, niobium, and nitrogen. It

also contains 20 wppm and 100 wppm of nickel and molybdenum, respectively.

Fig. 2 shows the decay heat generated in zone 1 as a function of time following shutdown. The ^{187}W isotope is even a larger contributor to the decay heat than activity generated following shutdown. It produces about 90% of the decay heat up to 1 day following shutdown. Similar to the induced activity, ^{185}W and ^{181}W dominate the induced decay heat in the period between 1 week and 1 year. ^{60}Co appears as nearly the sole contributor to the decay heat at 10 years after shutdown. ^{108m}Ag ($T_{1/2}$ = 130 y) produced by ^{107}Ag(n,γ) and ^{109}Ag(n,2n) reactions with the silver impurities (5 wppm) in the tungsten alloy is the major contributor to the decay heat after 100 years from shutdown. At times greater than 100 years, the decay heat is dominated by ^{39}Ar, ^{14}C, and ^{94}Nb ($T_{1/2}$ = 20,000 y) which is produced as a result of the ^{93}Nb(n,γ) and ^{94}Mo(n,p) reactions. The same nuclides dominate the activities and decay heat induced at all times following shutdown for both operational scenarios. It is clear that the results are nearly identical for short term activity and decay heat since the availability is the same during the last month of operation in both operation scenarios. On the other hand, the long term activity and decay heat determined by the total fluence is lower by about a factor of 3 for the M5 scenario. The activity and decay heat results for all the zones confirm this observation.

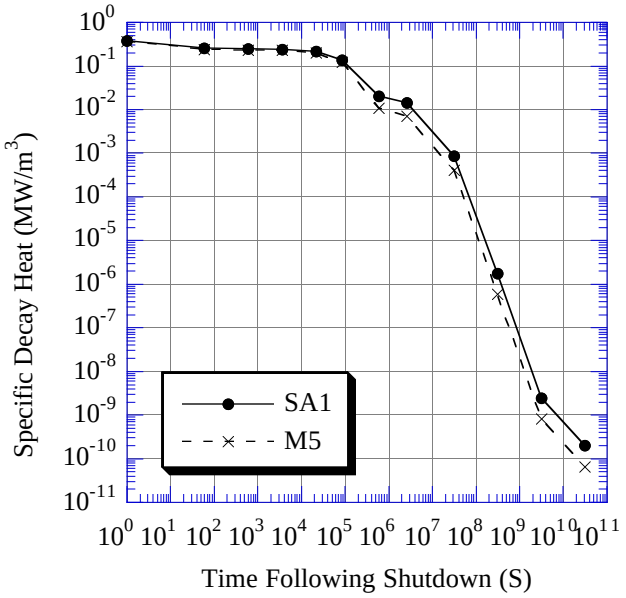

Fig. 2. Decay heat induced in dome W PFC (zone 1).

• Zone 2 (75% GlidCop Cu and 25% H_2O)

This zone represents the heat sink layer behind the tungsten. The copper isotopes, ^{64}Cu ($T_{1/2}$ = 12.71 h), ^{62}Cu ($T_{1/2}$ = 9.74 m), and ^{66}Cu ($T_{1/2}$ = 5.1 m) dominate the induced activity during the first hour following shutdown for both operational scenarios. ^{64}Cu continues to be the sole dominant isotope during the first few days. The three copper isotopes are produced by (n,γ) and (n,2n) interactions with the two stable copper isotopes, ^{63}Cu and ^{65}Cu. In addition, the ^{63}Cu(n,p) reaction results in the production of ^{63}Ni which dominates the induced activity for times greater than one week following shutdown, regardless of the pulsing scenario.

The decay heat generated in zone 2 after shutdown is dominated by the same 3 copper isotopes, ^{64}Cu, ^{62}Cu, and ^{66}Cu, during the first few days. Decay heat generated after the first week is mostly produced by impurities contained in the GlidCop Cu alloy. Except for ^{63}Ni, the decay heat for times greater than the first week is dominated by ^{60}Co up to ten years and ^{110m}Ag ($T_{1/2}$ = 252 d) up to a year. The ^{60}Co and ^{110m}Ag isotopes are produced by (n,γ) reactions with the two stable nuclides ^{59}Co and ^{109}Ag, respectively. The temporal variation of activity generated by the two operational scenarios is shown in Fig. 3.

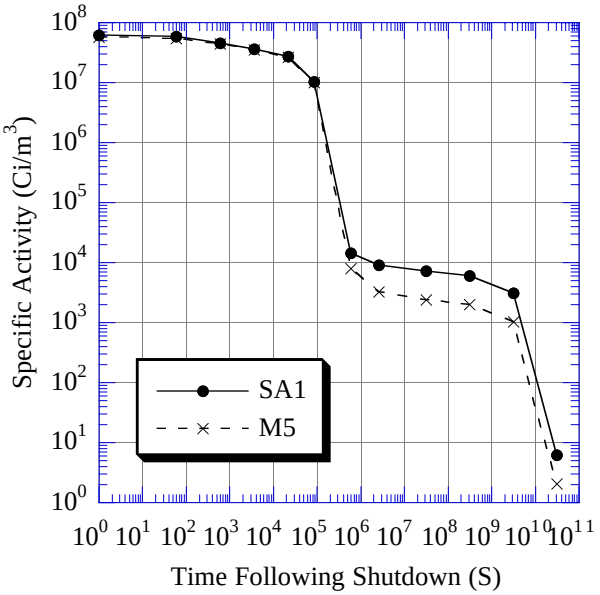

Fig. 3. Activity induced in dome PFC heat sink (zone 2).

b. Dome Body:

• Zone 1 (85% GlidCop Cu and 15% H_2O)

This zone represents the copper part of the dome body just behind the dome PFC. The activity and decay heat are dominated by radioactive products of the GlidCop Cu alloy. Radioisotopes dominating the activity and decay heat in zone 2 of the dome PFC are also, for the most part, the major contributors to this zone.

• Zone 2 (75% 316 SS-LN and 25% H_2O)

This zone represents the steel part of the dome body with highest flux exposure. Like most steel alloys, the activity and decay heat are dominated in short and mid-terms by the two manganese isotopes ^{56}Mn and ^{54}Mn. Fig. 4 shows the decay heat values generated in the zone. ^{56}Mn ($T_{1/2}$ = 2.58 h) is the major contributor to the activity and decay heat during the first few hours following shutdown. On the other hand, ^{54}Mn ($T_{1/2}$= 312.5 d) is the major contributor to the decay heat up to a year. Other contributors to activity are ^{51}Cr ($T_{1/2}$ = 27.71 d) during the first month, ^{55}Fe ($T_{1/2}$ = 2.7 y) during the first 10 years, ^{63}Ni during the first 100 years, and ^{59}Ni ($T_{1/2}$ = 80,000 y) for times more than 1000 years. The mid-term and long-term decay heat are generated by ^{58}Co ($T_{1/2}$ = 70.8 d) and ^{60}Co during the first year. ^{63}Ni dominated during the first 100 years. ^{59}Ni and ^{14}C dominate at 1000 years from shutdown.

The ^{51}Cr isotope is mostly produced by the ^{50}Cr(n,γ) and ^{52}Cr(n,2n) reactions. ^{55}Fe is a product of the ^{54}Fe(n,γ) and ^{56}Fe(n,2n) reactions. While ^{63}Ni is mainly produced by the ^{62}Ni(n,γ) reaction, ^{59}Ni could be produced by either of the ^{58}Ni(n,γ) or ^{60}Ni(n,2n) reactions. ^{58}Ni is also the major contributor to the production of ^{58}Co. The other contributor to the production of ^{58}Co is ^{59}Co which also produces ^{60}Co via the (n,γ) pathway. The ^{14}C isotope is produced by the ^{14}N(n,p) reaction.

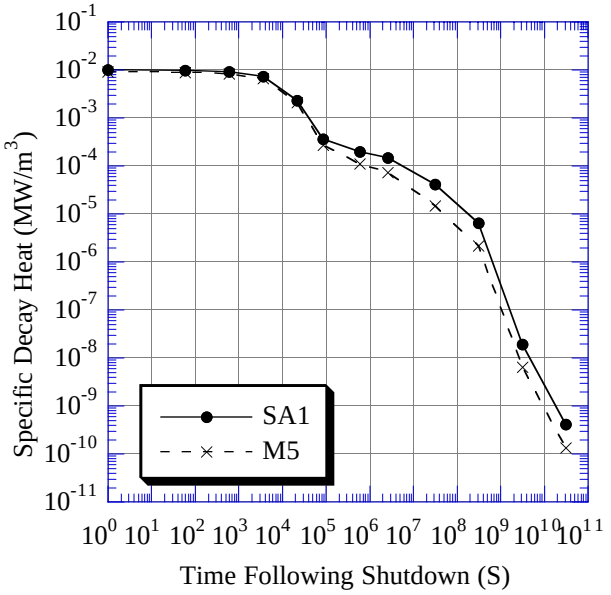

Fig. 4. Decay heat induced in zone 2 of the dome body.

c. Wings:

• Zone 1 and Zone 2 (16% W, 79% Cu and 5% H_2O)

Zones 1 and 2 represent the outer and inner wings of the divertor, respectively. Activities and decay heat values in both zones are dominated by the same radionuclides. ^{64}Cu and ^{187}W dominate the activity and decay heat during the first day following shutdown. ^{181}W and ^{185}W dominate during the first year. ^{60}Co and ^{63}Ni dominate at times greater than a year. Except for the tungsten isotopes, all other isotopes are the products of the GlidCop Cu alloy.

d. Outer Vertical Target:

• Zone 1 and Zone 2 (100% W)

These two zones represent the tungsten armor of the outer vertical target. The tungsten at the top of the outer vertical target (zone 1) experiences a higher level of activation in comparison to the lower part of the target (zone 2). The nuclides dominating the activity and decay heat are identical to those dominating the 1 cm tungsten layer of the dome's PFC.

• Zone 3 (89% C, 4% GlidCop Cu and 7% H_2O)

The zone represents the armor of the lower section of the outer vertical target. Carbon activity and decay heat are considerably low resulting in the copper alloy being the major source of activity and decay heat generated in the zone. ^{66}Cu and ^{64}Cu dominate during the first week after shutdown and ^{63}Ni dominates at longer times. ^{110m}Ag dominates the decay heat in the period between one week and one year.

e. Inner Vertical Target:

• Zone 1 and Zone 2 (100% W)

The zones represent the tungsten armor of the inner vertical target. Dominant nuclides are similar to zones 1 and 2 of the outer vertical target. Another similarity is apparent in the fact that tungsten experiences a higher level of activation and decay heat in the upper section of the inner vertical target (zone 1) than the level experienced by the lower section (zone 2).

• Zone 3 (89% C, 4% GlidCop Cu, and 7% H_2O)

This zone is similar to zone 3 of the outer vertical target. The levels of activity and decay heat generated in the inner vertical target are lower than the levels induced in the outer vertical target due to the fact that the inner vertical target is exposed to a lower neutron flux than the outer vertical target.

f. Cassette Body (80% 316 SS-LN and 20% H_2O):

Activity and decay heat were calculated for the different zones of the cassette body. This includes the central body, the inner leg, and the outer leg. As in zone 2 of the dome body, the activity and decay heat are dominated by the 316 SS-LN alloy. The activity and decay heat are dominated by the same isotopes mentioned in the previous discussion of zone 2 of the dome body. The levels of activity and decay heat generated in the inner leg are lower than the levels induced in the outer leg due

to the fact that the inner leg is exposed to a lower neutron flux.

g. Rails:

• Zone 1 and Zone 2 (100% 316 SS-LN)

The zones are made of 100% steel and hence, the manganese isotopes are the dominant source of activity and decay heat following shutdown. A detailed description of dominant nuclides is provided in the discussion of zone 2 of the dome body. The neutron flux in the rails is very small due to the shielding provided by the divertor cassette. As a result the activity and decay heat levels generated in the rails are extremely low, particularly for the outer rail (zone 1). Table I provides a summary of the peak specific activities and decay heat generated in key critical components of the divertor cassette at shutdown for the SA1 scenario.

Table I. Specific Activities and Decay Heat at Shutdown

Zone	Specific Activity (Ci/m^3)	Decay heat (MW/m^3)
Dome PFC	$1.58x10^8$	0.37
Dome Body	$4.33x10^7$	0.18
Outer Wings	$7.89x10^6$	$3.52x10^{-2}$
Inner Wings	$7.70x10^6$	$3.38x10^{-2}$
Outer Vertical Target	$1.21x10^8$	0.28
Inner Vertical Target	$7.29x10^7$	0.19

V. SUMMARY AND CONCLUSIONS

Three-dimensional activation analyses have been performed for the divertor region. A detailed 3-D model has been developed for the divertor region of the ITER Detailed Design. To examine the effect of pulsing sequences on the activity and decay heat generation, the calculations have been performed for two different operational scenarios. The first scenario (SA1) corresponds to a machine total fluence of 0.3 MWa/m^2 with a long term availability of 25% and a final month availability of 50%. A burn pulse length of one hour has been used in this scenario. The second scenario (M5) corresponds to a total fluence of 0.1 MWa/m^2. The M5 scenario has a long term availability of only 4% and a last month availability of 50%. A 1000 second burn pulse length is used for the M5 scenario. The short term activity and decay heat results are nearly identical since the availability is the same during the last month of operation in both operation scenarios. On the other hand, the long term activity and decay heat determined by the total fluence are lower by about a factor of 3 for the M5 scenario. Special attention has been given to the top 1 cm tungsten layer of the divertor dome. The radioactivity generated in the tungsten layers of the divertor are mostly dominated by ^{187}W during the first day after shutdown. Accurate calculation of the ^{187}W inventory that takes into account the self-shielding effect, also yielded accurate results for other radioisotopes produced by multi-step reactions with ^{187}W. The GlidCop copper and 316 SS-LN parts of the divertor also generated a considerable level of activity and decay heat. Nevertheless, the analysis showed that the tungsten PFC is clearly the most critical part of the divertor from a decay heat generation point of view.

ACKNOWLEDGMENTS

This report is an account of work performed under the Agreement among the European Atomic Energy Community, the Government of Japan, the Government of the Russian Federation, and the Government of the United States of America on Cooperation in the Engineering Design Activities for the International Thermonuclear Experimental Reactor ("ITER EDA Agreement") under the auspices of the International Atomic Energy Agency (IAEA).

REFERENCES

1. Technical Basis for the ITER Final Design Report, Cost Review and Safety Analysis, ITER EDA Documentation Series, International Atomic Energy Agency, Vienna, December 1997.

2. J. Briesmeister, Ed., "MCNP, A General Monte Carlo N-Particle Transport Code, Version 4A," LA-12625-M (1993).

3. R. MacFarlane, "FENDL/MC-1.0, Library of Continuous Energy Cross Sections in ACE Format for MCNP-4A," Summary Documentation by A. Pashchenko, H. Wienke and S. Ganesan, Report IAEA-NDS-169, Rev. 3, International Atomic Energy Agency (Nov. 1995).

4. J. Sisolak, Q. Wang, H. Khater and D. Henderson, "DKR-PULSAR2.0: A Radioactivity Calculation Code that Includes Pulsed/Intermittent Operation," to be published.

5. A. Pashchenko et al., "FENDL/A-2.0: Neutron Activation Cross-Section Data Library for Fusion Applications," Report INDC(NDS)-173, IAEA Nuclear Data Section, March 1997.

6. H. Y. Khater and M. E. Sawan, "Three-Dimensional Activation Analysis for the ITER Divertor Cassette," ITER/US97-IV-DV-12, ITER Technical Report (1997).